Spleen histology in children with sickle cell disease and hereditary spherocytosis: Hints on the disease pathophysiology

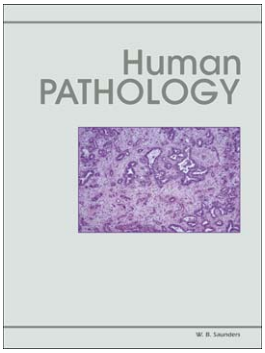

Spleen histology in children with sickle cell disease and hereditary spherocytosis: Hints on the disease pathophysiology

Marco Pizzi, Fabio Fuligni, Luisa Santoro, Elena Sabattini, Martina Ichino, Rita De Vito, Pietro Zucchetta, Raffaella Colombatti, Laura Sainati, Piergiorgio Gamba, Rita Alaggio

PII: S0046-8177(16)30253-2
DOI: doi: 10.1016/j.humpath.2016.09.028
Reference: YHUPA 4030

To appear in: *Human Pathology*

Received date: 4 May 2016
Revised date: 17 September 2016
Accepted date: 20 September 2016

Please cite this article as: Pizzi Marco, Fuligni Fabio, Santoro Luisa, Sabattini Elena, Ichino Martina, De Vito Rita, Zucchetta Pietro, Colombatti Raffaella, Sainati Laura, Gamba Piergiorgio, Alaggio Rita, Spleen histology in children with sickle cell disease and hereditary spherocytosis: Hints on the disease pathophysiology, *Human Pathology* (2016), doi: 10.1016/j.humpath.2016.09.028

Spleen histology in children with sickle cell disease and hereditary spherocytosis: Hints on the disease pathophysiology

Marco Pizzi[1], Fabio Fuligni[2], Luisa Santoro[1], Elena Sabattini[3], Martina Ichino[4], Rita De Vito[5], Pietro Zucchetta[6], Raffaella Colombatti[7], Laura Sainati[7], Piergiorgio Gamba[4], Rita Alaggio[1]

Affiliations

1. Surgical Pathology and Cytopathology Unit, Department of Medicine-DIMED, University of Padova, Padova, Italy
2. Department of Genetics and Genome Biology, The Hospital for Sick Children, Toronto (ON), Canada
3. Hematopathology Unit, Sant'Orsola/Malpighi Hospital, Bologna, Italy
4. Pediatric Surgery Unit, Department of Woman and Child Health, University of Padova, Padova, Italy
5. Department of Pathology, Bambino Gesù Children's Hospital, Rome, Italy
6. Nuclear Medicine Service, Department of Medicine-DIMED, University of Padova, Padova, Italy
7. Clinic of Pediatric Hematology/Oncology, Department of Woman and Child Health, University of Padova, Padova, Italy

Word Count: 3398 (not including the abstract)

Figures: 4

Tables: 2

Short title: Spleen histology in SCD and HS

List of Abbreviations: HS= hereditary spherocytosis; LF= lymphoid follicle; MZ= marginal zone; PCA= principal component analysis; RBC= red blood cell; SCD= sickle-cell disease; SMA= smooth muscle actin

Corresponding Author: Rita ALAGGIO, MD, General Pathology & Cytopathology Unit, Department of Medicine-DIMED, University of Padova; via Gabelli 61, 35121 Padova (PD), Italy. Phone: +39 049 8211317. Fax: 049 8212277. e-mail: ral@unipd.it

Financial Disclosure Statement: no Financial Conflicts to declare

Abstract

Hereditary spherocytosis (HS) and sickle cell disease (SCD) are associated with splenomegaly and spleen dysfunction in pediatric patients. Scant data exist on possible correlations between spleen morphology and function in HS and SCD. This study aimed to assess the histological and morphometric features of HS and SCD spleens, in order to get possible correlations with disease pathophysiology. In a large series of spleens from SCD, HS and control patients the following parameters were considered: (i) macroscopic features; (ii) lymphoid follicle (LF) density; (iii) presence of peri-follicular marginal zones (MZs); (iv) presence of Gamna-Gandy bodies; (v) density of CD8-positive sinusoids; (vi) density of CD34-positive microvessels; (vii) presence/distribution of fibrosis and SMA-positive myoid cells; (viii) density of CD68-positive macrophages. SCD and HS spleens have similar macroscopic features. SCD spleens had lower LF density and fewer MZs than HS spleens and controls. SCD also showed lower CD8-positive sinusoid density, increased CD34-positive microvessel density and SMA-positive myoid cells, and higher prevalence of fibrosis and Gamna-Gandy bodies. HS had lower LF and CD8-positive sinusoid density than controls. No significant differences were noted in red pulp macrophages. By multivariate analysis, the majority of HS spleens clustered with controls, while SCD grouped separately. A multi-parametric score could predict the degree of spleen changes irrespective of the underlying disease. In conclusion, SCD spleens display greater histologic effacement than HS and SCD-related changes suggest impaired function due to vascular damage. These observations may contribute to guide the clinical management of patients.

Keywords: Hereditary spherocytosis; Sickle cell disease; Spleen; Vasculopathy

Funding: This research did not receive any specific grant from funding agencies in the public, commercial, or not-for-profit sectors.

1. Introduction

The spleen is the largest organ of the lymphatic and reticuloendothelial system and its functions include blood cell storage, hemocatheresis and immune response against blood-borne infections (1). These functions are sustained by two topographically and functionally distinct compartments: the white pulp and the red pulp (2).

The white pulp consists of periarterial sheaths of lymphocytes with evenly distributed lymphoid follicles (LFs). Both primary and secondary LFs display an outer marginal zone (MZ), composed of small to medium size lymphocytes with abundant cytoplasm. MZ lymphocytes exert a pivotal role in immune responses against polysaccharide-encapsuled bacteria (i.e. *S. pneumoniae*, *N. meningitidis* and *H. influenzae*) (3-5). The red pulp consists of sinusoids surrounded by a meshwork of macrophages with interlacing cytoplasmic processes (red pulp cords). The histological and ultra-structural features of the red pulp allow the filtration of circulating blood cells and the removal of senescent and/or damaged erythrocytes (1, 2).

Several hematological disorders can alter the microscopic features of the spleen, with consequent damage to its immunologic and non-immunologic functions. Hereditary spherocytosis (HS) and sickle cells disease (SCD) are rare congenital diseases, characterized by distinct pathogenic mechanisms and associated with variable spleen dysfunction (6, 7). HS is a genetic disorder of the erythrocyte cytoskeleton, causing abnormal red blood cell (RBC) shape, loss of RBC membrane and chronic hemolysis (8). The spleen is the main site of RBCs disruption, as spherocytes can hardly squeeze through the splenic sinusoids and are entrapped in the red pulp cords (1). This causes moderate to severe splenomegaly, which is typically associated with anemia, reticulocytosis, jaundice and increased risk of gallstones. Splenectomy improves HS-related symptoms in the majority of cases (6, 9).

SCD is a hereditary disorder caused by a point mutation on the *β-globin* gene, inducing a glutamic acid to valine substitution at position 6 (10). The resulting hemoglobin (i.e. hemoglobin S [HbS]) is characterized by peculiar biochemical properties. It indeed displays a hydrophobic motif, which prompts the aggregation and precipitation of de-oxygenated hemoglobins in RBCs (11). The precipitates promote the acquisition of a sickle-like shape, induce RBC hemolysis and cause the entrapment of sickle cells in small vessels and capillary networks (12). This leads to both intra-vascular and extra-vascular hemolysis, with vaso-occusive crises, microvascular thrombosis and ischemic damage to several organs. SCD is indeed characterized by a broad spectrum of clinical manifestations, including pain crises, renal papillary necrosis, ischemic strokes and bacterial infections. The latter are supposed to be mainly caused by the progressive shrinking of the spleen (i.e. functional asplenia) possibly due to recurrent ischemic accidents of the red pulp (7). In SCD, the spleen can also be involved by acute sequestration crises, which are characterized by a precipitous drop in hemoglobin concentration, reticulocytosis and tender splenomegaly (13, 14).

The morphological and pathophysiological bases of spleen dysfunction in HS and SCD are not fully described. Their better understanding may however contribute to improve the clinical management of patients. In the present study, the histological features of HS and SCD spleens have been characterized by thorough morphometric and immunohistochemical analysis. The histological results also allowed the develpment of a multi-parametric score to assess the severity of splenic changes in each single case.

2. Materials & Methods

2.1 Case selection

This retrospective, multi-institutional study considered a series of 42 spleens from pediatric patients (mean age: 8.6 years; M:F ratio: 1.2) with HS and SCD, who underwent partial or total

splenectomy for disease-related splenomegaly/hypersplenism. In detail, the following cases were considered: (i) 35 spleens from children with HS (total splenectomy: 32 cases; partial splenectomy: 3 cases); (ii) 7 spleens from children with SCD (total splenectomy in all cases; all spleens were removed as a consequence of previous sequestration crises); (iii) 10 control spleens removed for traumatic rupture in pediatric patients (total splenectomy in all cases). The gross description (spleen weight; presence of sub-capsular infarcts; thrombosis of hilar vessels) and clinic-epidemiological data were available in all cases (Table 1).

Paraffin embedded tissue blocks were retrieved from the archives of the Surgical Pathology & Cytopathology Unit of Padova University Hospital (Padova, Itay), the Hematopathology Unit of Bologna University Hospital (Bologna, Italy) and the Ospedale Pediatrico Bambino Gesù (Rome, Italy). All cases were reviewed by two pathologists (LS and MP) and representative tissue sections were selected for morphometric and immunohistochemical analyses. The ethic regulations on research on human tissues were followed by each of the participating Centers, consistent with the declaration of Helsinki.

2.2 Histologic evaluation of the spleen

Representative formalin-fixed, paraffin-embedded tissue blocks were assessed for the following morphological and morphometric parameters: (i) white pulp architecture and LF density (i.e. number of LFs per square unit); (ii) presence/absence of a peri-follicular MZ; (iii) presence of Gamna-Gandy bodies (i.e. sclero-siderotic nodules); (iv) presence of splenic fibrosis (assessed by reticulin stain and defined as the presence of reticulin fibers exceeding those normally observed around splenic vessels and red pulp sinusoids); (v) density of CD8-positive sinusoids (i.e. mean number of cross-sectioned CD8-positive vessels per 10 high-power fields); (vi) density of CD34-positive red pulp vessels (i.e. mean number of cross-sectioned CD34-postive vessels per 10 high-power fields); (vii) density of CD68-positive red pulp macrophages (mean number of CD68-postive cells per 10 high-power fields); (viii) presence and distribution of SMA-positive myoid cells.

The morphometric parameters (i.e. FL density, CD8-positive vessel density, CD34-positive vessel density, and CD68-positive macrophage density) were manually evaluated using the DMD108 Digital Micro-imaging Device and Software (Leica Microsystems, Milano, Italy).

2.3 Immunohistochemical analysis

Splenic stroma and red pulp vessels were immunohistochemically studied with primary antibodies against the following antigens: (i) CD34 (clone QBEnd/10, Leica; Newcastle, United Kingdom); (ii) CD8 (clone C8/144B, Dako; Glostrup, Denmark); (iii) Smooth Muscle Actin (SMA, clone 1A4, Dako); (vi) CD68 (clone PGM1, Dako). Antigen detection was performed using an automated immunostainer (Bond-maX; Leica, Newcastle Upon Tyne, UK), as previously described (15). In SCD and HS cases, the number of SMA-positive stromal cells was assessed by comparison with control spleens and graded as increased, normal, or reduced.

2.4 Statistical analysis

Comparison of the histological variables was performed by both univariate and multivariate analyses using IBM Spss Statistics 20.0 (IBM, Armonk, USA). For univariate analysis, differences among groups were evaluated by the Fisher's exact test (qualitative variables) and the Student t-test (quantitative variables). Differences were considered statistically significant for values of $p< 0.05$.

Multivariate analysis was performed using the histological variables, which were statistically different by univariate analysis. The principal component analysis (PCA) was applied to reduce the number of observed parameters, creating a list of factors (components) as a linear combinations of the original variables. The total amount of variance explained by the first 3 principal components is 84.1%.

K-mean cluster analysis was used to stratify and classify the spleens according to the histological findings (16). Briefly, K-mean cluster algorithm iteratively evaluates the cluster center for every histological variable and assigns every sample to the closest cluster, according to the

Euclidean distance between each observed histological value and its relative cluster center. Each variable was thus given a dichotomic value (0 *versus* 1), based on thresholds defined by a k-means clustering algorithm (Table 2). The sum of such values was then calculated and cases were clustered according to the obtained score. The results were graphically represented by a heatmap using MeV v4.7.4 software (17).

3. Results

3.1 Macroscopic and histological features of HS spleens

Among children with HS (mean age: 8.72 years; M:F ratio: 0.9), the spleens removed by total splenectomy were significantly larger than controls (mean spleen weight: 381.3 g in the HS subgroup; 130.6 g in the control subgroup) (Student's t-test, $p<0.01$). Gross examination did not reveal sub-capsular infarcts and/or thrombosis of the hilar vessels.

Histological examination of HS spleens disclosed preserved white pulp architecture, with primary and secondary follicles surrounded by a clear-cut MZ (34/35 cases). HS spleens were however characterized by a lower LF density compared to controls (mean LF density: 0.3/mm^2 in HS spleens; 0.6/mm^2 in control spleens) (Student's t-test, $p<0.01$) (Figure 1; Table 1).

The majority of HS spleens had preserved red pulp architecture, with no evidence of fibrosis and/or Gamna-Gandy bodies. Similar results were reported in control spleens (Fisher's exact test; no statistically significant differences) (Figure1; Table 1). Of note, HS was characterized by decreased numbers of CD8-positive sinusoids compared to normal controls (mean sinusoid density: 47.3/HPF in HS; 57.4/HPF in normal spleens) (Student's t-test, $p<0.01$). Differences in CD34-positive microvessels were not statistically significant (mean microvessel density: 43.5/HPF in HS; 45.2/HPF in normal spleens) (Student's t-test, $p=0.38$) (Table 1; Figure 2). In 33/35 HS cases, the number and distribution of SMA-positive myoid cells overlapped the pattern observed in normal controls. An increase of SMA-positive myoid cells was only documented in 2 cases, which were

also characterized by red pulp fibrosis. In these cases, the distribution of SMA-positive myoid cells roughly paralleled the extent and distribution of reticulin fibers (Figure 2). No significant differences in the density of CD68-positive macrophages were noted between HS spleens and control cases (mean macrophage density: 64.1/HPF in HS; 65.3/HPF in normal spleens) (Student's t-test, p=0.49).

3.2 Macroscopic and histological features of SCD spleens

SCD cases included 7 children, who underwent total splenectomy for disease-related complications (mean age at splenectomy: 6.4 years; M:F ratio: 2.0). The mean weight of SCD spleens (427.6 g) was significantly higher than in normal controls (Student's t-test, $p<0.01$). On gross examination, there was no evidence of infarcts and/or thrombosis of the hilar vessels.

Histologic examination disclosed marked alterations of the white pulp, with only scattered lymphoid follicles, mostly devoid of well-formed MZs (mean LF density: 0.1/mm^2; presence of MZ: 2/7 cases). Differences in white pulp architecture between SCD and control spleens were statistically significant (Student's t-test and Fisher's exact test, $p<0.01$) (Figure 1; Table 1).

SCD spleens also disclosed marked alteration of the red pulp, with increased reticulin deposition in 6/7 cases. Gamna-Gandy bodies were present in all the examined samples. The density of CD8-positive sinusoids in SCD was markedly reduced compared to normal controls (mean sinusoid density in SCD: 26.2/HPF) (Student's t-test, $p<0.01$). Conversely, the number of CD34-positive microvessels was higher in SCD than control spleens (mean CD34-positive microvessel density: 64.3/HPF in SCD) (Student's t-test, p=0.05). Overall, 6/7 SCD spleens disclosed a significant increase of SMA-positive myoid cells compared to controls (Fisher exact tests, $p<0.01$) (Table 1; Figure 2). Like in HS, the number and distribution of SMA-positive myoid

cells paralleled reticulin fibrosis. Similar CD68-positive cell density was reported between SCD and control spleens (mean macrophage density: 66.0/HPF in SCD) (Student's t-test, p=0.88).

3.2 Comparison between HS and SCD spleens

By univariate analysis, SCD disclosed lower LF density and less MZ formation than HS spleens (Student's t-test and Fisher's exact test, $p<0.01$). SCD spleens featured higher incidence of red pulp fibrosis and Gamna-Gandy bodies (Fisher's exact test, $p<0.01$). They were also characterized by lower CD8-positive sinusoid density and higher CD34-positive microvessel density (Student's t-test, $p<0.05$; Figure 3). An increase of SMA-positive myoid cells was more frequently observed in SCD than HS (Fisher's exact test, $p<0.01$; Figure 3), while no differences in CD68-positive cell density were noted (Fisher's exact test, p=0.51) (Table 1).

The overall histological features of SCD, HS and control spleens were also evaluated by means of PCA, a multivariate procedure clustering cases according to a linear combination of histological parameters. This analysis disclosed sharply distinct grouping of HS and SCD spleens. In particular, all but 2 HS spleens clustered in close proximity to control spleens. On the contrary, SCD spleens formed a distinct group, which also included the 2 outlier cases of HS (Figure 4A).

Taken together, these results demonstrate that HS and SCD spleens have distinct histological features at both univariate and multivariate analysis. The latter also demonstrates that the overall histological features of HS spleens are closer to normal controls than SCD.

3.3 Multi-parametric score to predict the severity of spleen histological changes

The finding that HS and SCD spleens form sharply distinct clusters with occasional outliers prompted us to develop a histologic score to assess the severity of the splenic changes, irrespective of the original diagnosis. This score would objectively stratify spleens based on their deviation from normal controls and may prove useful for both research and clinical purposes.

The score was calculated using a k-mean clustering algorithm (Table 2) and the obtained results were clustered accordingly (Figure 4B). This statistical procedure revealed that scores ≥3 predict marked deviation from controls and are thus suggestive of severe spleen damage. In particular, high scores were reported in all SCD (score= 7: 4 cases; score= 6: 1 case; score= 4: 1 case; score= 3: 1 case), and in 2 HS (score= 3) spleens. Low scores were instead reported in 33 HS (score=1 in 1 case; score= 0 in 32 cases) and in all controls (score= 0 in all cases).

5. Discussion

HS and SCD are congenital hematological disorders with different etiological and pathophysiological features. Seminal studies have investigated the morphological features of the spleen in HS and SCD, disclosing a reduction of the white pulp and variable congestion of the red pulp (1, 2, 18-24). SCD (but not HS) has also been associated with sub-capsular infarcts and sclero-siderotic nodules of the red pulp (i.e. Gamna-Gandy bodies) (1, 25). Of note, the majority of such studies was performed before the introduction of immunohistochemical techniques and lacked a thorough characterization of the splenic anatomic and functional components. Based on this preliminary evidence, the present study aimed to investigate the morphological, immunohistochemical and morphometric changes of a series of HS and SCD.

Spleens in children with HS and SCD were markedly enlarged compared to controls, but did not show any focal lesion and/or major vascular thrombosis. Such a significantly increased volume is probably attributable to marked red pulp congestion (i.e. spherocyte entrapment within red pulp sinusoids in HS; marked red pulp congestion due to prior sequestration crises in SCD). At histology, SCD spleens were characterized by significant alteration of the white pulp, with low LF density and absence of MZs in the majority of cases. The decreased LF density could at least partially be explained by the congestion and expansion of the red pulp sinusoids. On the other hand, the absence of well-formed MZs in SCD is in keeping with the clinical observation of impaired immunologic

functions against bloodborne bacteria (7). The latter may also be related to severe impairment of red pulp vessels, which exert a pivotal role in blood filtration and bacteria culling.

SCD was indeed associated with reduced CD8-positive sinusoid density, increased CD34-positive microvessel density, higher incidence of red pulp fibrosis and Gamna-Gandy bodies (Table 1; Figure 1 and Figure 2). The distribution of SMA-positive myoid cells paralleled the extent of fibrosis, indicating a possible role for these cells in the deposition of reticulin fibers. These findings suggest the occurrence of chronic micro-vascular accidents within the red pulp (thrombosis and/or vasculopathy), ultimately leading to effacement of the red pulp vessels and to the development of red pulp fibrosis. Vasculopathy is indeed a well known pathogenic mechanism of SCD-related organ damage, being responsible of brain, lung and kidney dysfunction (26-29). Our findings may imply the importance of these changes even for SCD-related spleen impairment. The young age of our patients also suggests that such pathogenic events occur very early in the natural history of the disease.

HS spleens were characterized by less severe histological derangements. The white pulp indeed disclosed normal lymphoid cuffs, with well-preserved LFs and clear-cut MZs. This observation is in keeping with previously reported data, which documented the preservation of the lymphoid architecture in HS spleens (1). Of note, our study also disclosed a reduction of FL density and CD8-positive sinusoids in HS (Table 1; Figure 1 and 2). Such observations (never reported before) may indicate some impairment of spleen physiology in HS. The degree of these changes seems however too small to bear any clinical consequence.

No differences were noted in the number of red pulp macrophages among HS, SCD and control spleens. This finding contrasts with previous ultra-structural studies, reporting increased splenic cord macrophages in HS compared to normal spleens (19, 22). Such a discrepancy may be in part related to the use of different techniques (CD68 immunohistochemistry on whole tissue sections *versus* electron microscopy on small splenic samples), but further studies are needed to clarify this issue. In this context, it may also be useful to correlate the histological findings with the

results of nuclear imaging studies (i.e. ^{99m}Tc-labeled sulfur-colloid test and/or ^{99m}Tc-labeled heat-damaged red blood cells test) (30). This would indeed contribute to better characterize the morphological-functional status of the reticuloendothelial system in HS and SCD spleens.

From a pathogenic perspective, the SCD-induced red pulp effacement deserves special consideration. SCD is a chronic hemolytic disorder characterized by severe vascular damage and widespread endothelial injury (7, 31). One of the key mediators of such processes is free serum heme, which is released from HbS upon sickle cell lysis (32, 33). Free serum heme binds to surface TLR4 of endothelial cells and triggers a cascade of deranged signaling pathways, which ultimately lead to endothelial cell dysfunction and vasculopathy (32). In SCD, it is thus conceivable that chronic vascular occlusion, RBC hemolysis, and heme release induce severe injury of the splenic sinusoids, with red pulp fibrosis and proliferation of non-specialized CD34-positive microvessels. This hypothesis may also explain the less severe changes observed in HS. Pure HS is indeed characterized by un-mutated hemoglobin genes, which are significantly less prone to release free heme after RBC lysis (31, 32, 34).

The observation of severe spleen damage in a small subset of HS patients led us to develop a multi-parametric score to assess the severity of spleen damage irrespective of the underlying disease (Table 2; Figure 4B). This score effectively stratified spleens according to reproducible and easily assessable parameters and may prove useful for both research and clinical purposes.

As for its research applications, the histological score would enable to objectively grade the severity of spleen impairment, allowing the comparison with other clinical, laboratory and/or radiological data. It may thus contribute to better delineate the pathophysiology and clinical-pathological correlations of several spleen disorders. From a clinical perspective, this score may impact on the management of patients in specific clinical settings, such as after partial splenectomy. In this context, the grading of spleen changes may indeed help assess the morphological-functional status of the residual spleen, thus allowing the planning of adequate post-surgical therapies. Such

clinical applications are however still speculative and need to be investigated by future clinical-pathological studies.

In conclusion, this study demonstrates different patterns of spleen damage in HS and SCD. These differences may result from diverse pathogenic mechanisms (extra-vascular hemolysis in HS; intra-/extra-vascular hemolysis and microvascular damage in SCD) and may provide hints for the management of patients. The development of a multi-parametric score to assess spleen effacement contributes to this aim and represents a tool for future research on spleen dysfunction in hematological and non-hematological disorders.

FIGURE LEGENDS

Figure 1. Histological features of HS, SCD and control spleens.

A-C. The spleens from patients with HS were characterized by preservation of the white pulp, with well-preserved marginal zones (**A**). The red pulp was congested (**B**) with no evidence of reticulin fiber deposition (**C**).

D-F. The spleens from patients with SCD disclosed altered lymphoid follicles (i.e. reduced density; absence of marginal zones) (**D**), numerous Gamna-Gandy bodies (**E**) and red pulp fibrosis (**F**).

G-I. Control spleens showed well-developed secondary follicles, with clear-cut marginal zones (**G**). The red pulp was unremarkable, with no increase in reticulin fibers (**H-I**). (H&E and Reticulin stain; original magnification, x20).

Figure 2. Immunohistochemical features of HS, SCD and control spleens.

A-C. The spleens from patients with HS were characterized by a slight reduction of CD8-positive red pulp sinusoid (**A**) and by a normal distribution of CD34-positive microvessels (**B**). In the majority of cases, SMA-positive myoid cells were normally represented (**C**).

D-F. SCD spleens disclosed a sharp reduction of CD8-positive sinusoids (**D**), with a parallel increase of both CD34-positive microvessels (**E**) and SMA-positive myoid cells (**F**).

G-I. Control spleens showed a dense network of CD8-positive sinusoids (**G**), with sparse CD34-positive microvessels (**H**) and SMA-positive myoid cells (**I**). (Peroxidase stain; original magnification, x20).

Figure 3. Comparison of the histological features in the studied spleens.

A-C. Univariate analysis disclosed significantly higher lymphoid follicle (LF) density (**A**) and CD8-positive sinusoid density (**B**) in control spleens compared to both SCD and HS spleens. CD34-positive microvessels were more abundant in SCD than in HS and controls (**C**) (Student's t-test). **D-F**. Marginal zones were more frequently documented in HS and control spleens compared to SCD (**D**). By contrast, Gamna-Gandy bodies and red pulp fibrosis were more frequent in SCD (the blotted values refer to the percentage of positive and negative cases for each group; Fisher exact test) (Notes: * $p<0.01$; ** $p<0.05$).

Figure 4. Multivariate analysis of the histological features in the studied spleens.

A. Primary component analysis clustered the spleens according to a linear combination of histological parameters. The analysis disclosed that the majority of HS grouped together with controls, while all SCD and 2 HS spleens formed a distinct cluster.

B. K-mean cluster analysis was applied to classify the spleens, irrespective to the original diagnosis. Each case was stratified according to dichotomic values attributed to the histological variables (red square: score 1; green square: score 0). The combination of such values led to the identification of 2 sharply distinct clusters: one (left side of the plot) grouped all the control spleens and the majority of HS cases; the other (right side of the plot) grouped 6/7 SCD spleens and 2 outlier HS. In the heatmap, each row represents a histological parameter and each column represents a sample.

References

1. Neiman RS, Orazi A, Wolf BC. Disorders of the spleen. 2nd ed. W.B. Saunders: Philadelphia, 1999. xiv, 294 p., 10 p. of plates pp.

2. Bishop MB, Lansing LS. The spleen: a correlative overview of normal and pathologic anatomy. Hum Pathol 1982;13:334-42.

3. Zandvoort A, Timens W. The dual function of the splenic marginal zone: essential for initiation of anti-TI-2 responses but also vital in the general first-line defense against blood-borne antigens. Clin Exp Immunol 2002;130:4-11.

4. Martin F, Kearney JF. Marginal-zone B cells. Nat Rev Immunol 2002;2:323-35.

5. Szczepanek SM, McNamara JT, Secor ER, Jr., *et al.* Splenic morphological changes are accompanied by altered baseline immunity in a mouse model of sickle-cell disease. Am J Pathol 2012;181:1725-34.

6. Perrotta S, Gallagher PG, Mohandas N. Hereditary spherocytosis. Lancet 2008;372:1411-26.

7. Rees DC, Williams TN, Gladwin MT. Sickle-cell disease. Lancet 2010;376:2018-31.

8. Delaunay J. The molecular basis of hereditary red cell membrane disorders. Blood Rev 2007;21:1-20.

9. Eber SW, Armbrust R, Schroter W. Variable clinical severity of hereditary spherocytosis: relation to erythrocytic spectrin concentration, osmotic fragility, and autohemolysis. J Pediatr 1990;117:409-16.

10. Bunn HF. Pathogenesis and treatment of sickle cell disease. N Engl J Med 1997;337:762-9.

11. Brittenham GM, Schechter AN, Noguchi CT. Hemoglobin S polymerization: primary determinant of the hemolytic and clinical severity of the sickling syndromes. Blood 1985;65:183-9.

12. Zhang D, Xu C, Manwani D, Frenette PS. Neutrophils, platelets, and inflammatory pathways, at the nexus of sickle cell disease pathophysiology. Blood 2016.

13. Khatib R, Rabah R, Sarnaik SA. The spleen in the sickling disorders: an update. Pediatr Radiol 2009;39:17-22.

14. Brousse V, Buffet P, Rees D. The spleen and sickle cell disease: the sick(led) spleen. Br J Haematol 2014;166:165-76.

15. Pizzi M, Piazza F, Agostinelli C, *et al.* Protein kinase CK2 is widely expressed in follicular, Burkitt and diffuse large B-cell lymphomas and propels malignant B-cell growth. Oncotarget 2015;6:6544-52.

16. Hartigan JA. Clustering algorithms. Wiley: New York,, 1975. xiii, 351 p. pp.

17. Saeed AI, Sharov V, White J, *et al.* TM4: a free, open-source system for microarray data management and analysis. Biotechniques 2003;34:374-8.

18. Bosman C, Cavaliere P. Biometrically revealed splenic differences between thalassemia, hereditary spherocytosis and elliptocytosis. Pathol Microbiol (Basel) 1967;30:35-58.

19. Molnar Z, Rappaport H. Fine structure of the red pulp of the spleen in hereditary spherocytosis. Blood 1972;39:81-98.

20. Breitfeld V, Lee RE. Pathology of the spleen in hematologic disease. Surg Clin North Am 1975;55:233-51.

21. Myhre Jensen O, Kristensen J. Red pulp of the spleen in autoimmune haemolytic anaemia and hereditary spherocytosis: morphometric light and electron microscopy studies. Scand J Haematol 1986;36:263-6.

22. Ferreira JA, Feliu E, Rozman C, *et al.* Morphologic and morphometric light and electron microscopic studies of the spleen in patients with hereditary spherocytosis and autoimmune haemolytic anaemia. Br J Haematol 1989;72:246-53.

23. Bauer JT. Siderofibrosis of the spleen secondary to sickle-cell anemia (three case reports. Bull Phila Pa Hosp Ayer Clin Lab 1946;3:477-82.

24. Diggs WL. Siderofibrosis of the spleen in sickle cell anemia. JAMA 1935;104:538-41.

25. Piccin A, Rizkalla H, Smith O, *et al.* Composition and significance of splenic Gamna-Gandy bodies in sickle cell anemia. Hum Pathol 2012;43:1028-36.

26. Platt OS. Sickle cell anemia as an inflammatory disease. J Clin Invest 2000;106:337-8.

27. Nath KA, Hebbel RP. Sickle cell disease: renal manifestations and mechanisms. Nat Rev Nephrol 2015;11:161-71.

28. Novelli E, Gladwin MT. Crises in Sickle Cell Disease. Chest 2015.

29. Rothman SM, Fulling KH, Nelson JS. Sickle cell anemia and central nervous system infarction: a neuropathological study. Ann Neurol 1986;20:684-90.

30. de Porto AP, Lammers AJ, Bennink RJ, *et al.* Assessment of splenic function. Eur J Clin Microbiol Infect Dis 2010;29:1465-73.

31. Reiter CD, Wang X, Tanus-Santos JE, *et al.* Cell-free hemoglobin limits nitric oxide bioavailability in sickle-cell disease. Nat Med 2002;8:1383-9.

32. Belcher JD, Chen C, Nguyen J, *et al.* Heme triggers TLR4 signaling leading to endothelial cell activation and vaso-occlusion in murine sickle cell disease. Blood 2014;123:377-90.

33. Camus SM, De Moraes JA, Bonnin P, *et al.* Circulating cell membrane microparticles transfer heme to endothelial cells and trigger vasoocclusions in sickle cell disease. Blood 2015;125:3805-14.

34. Bunn HF, Jandl JH. Exchange of heme among hemoglobins and between hemoglobin and albumin. J Biol Chem 1968;243:465-75.

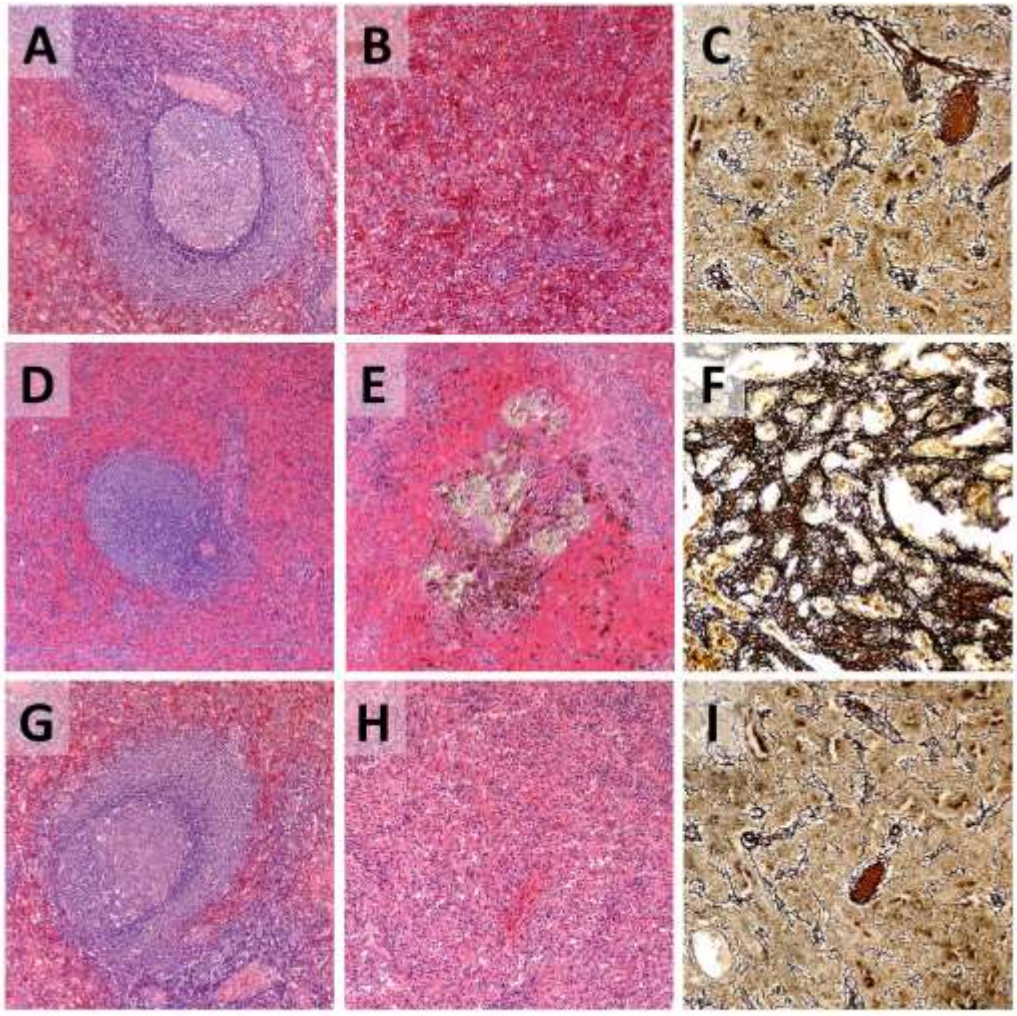

Pizzi M *et al* – Figure 1

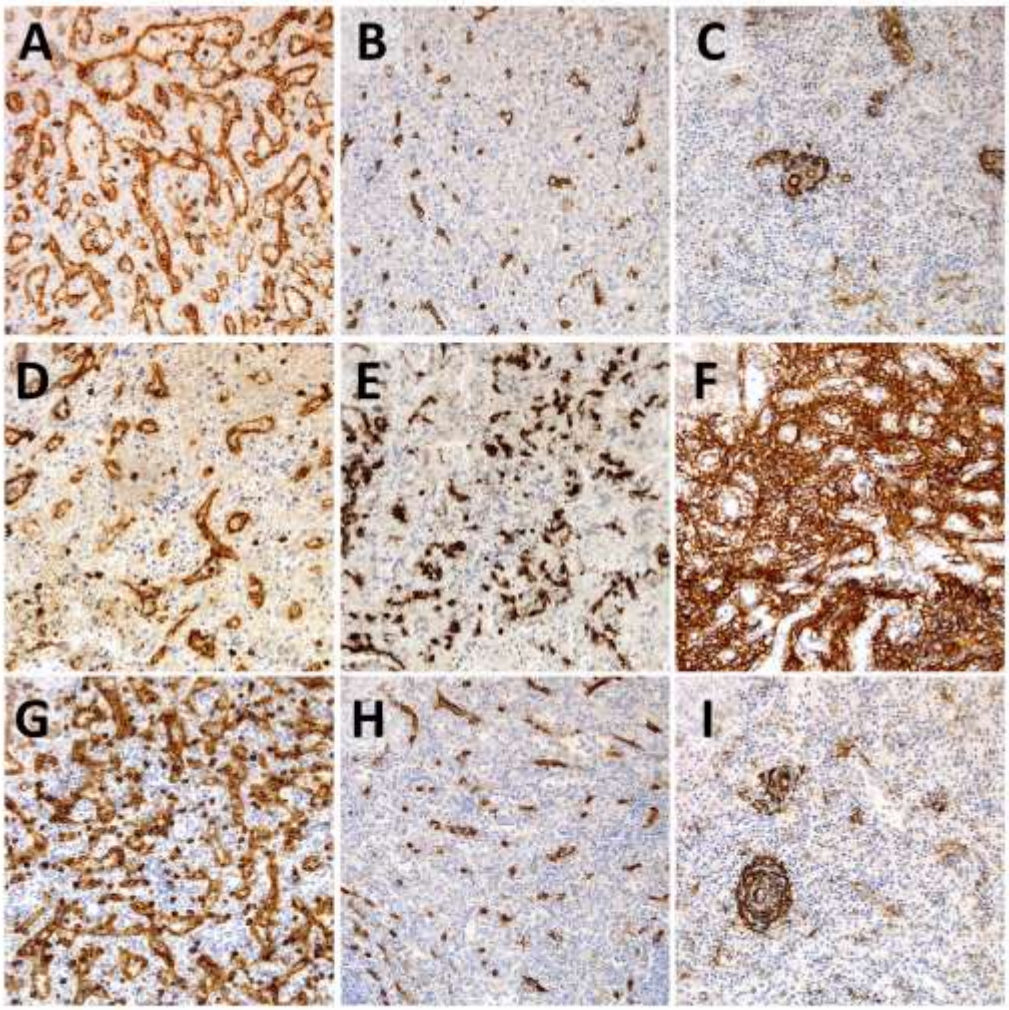

Pizzi M *et al* – Figure 2

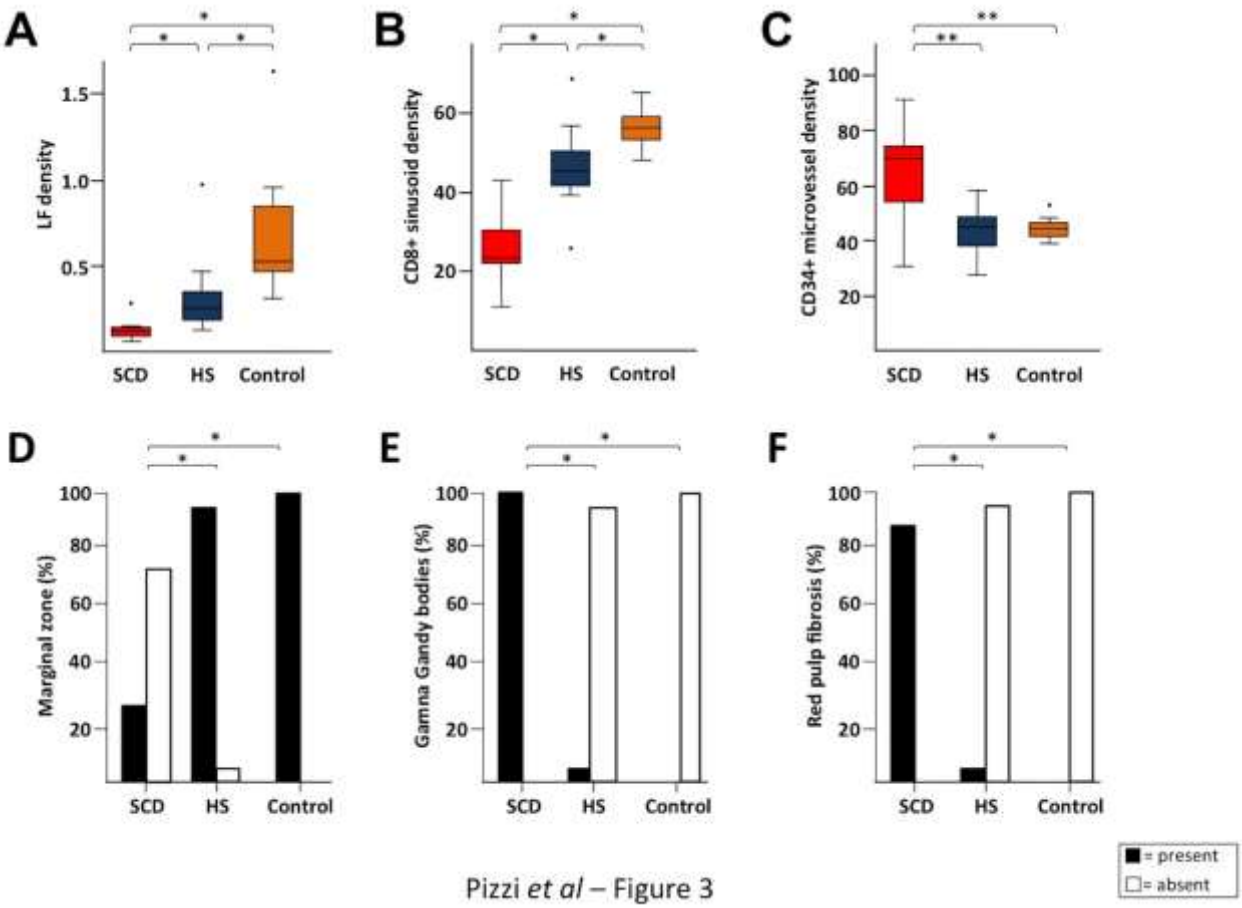

Pizzi *et al* – Figure 3

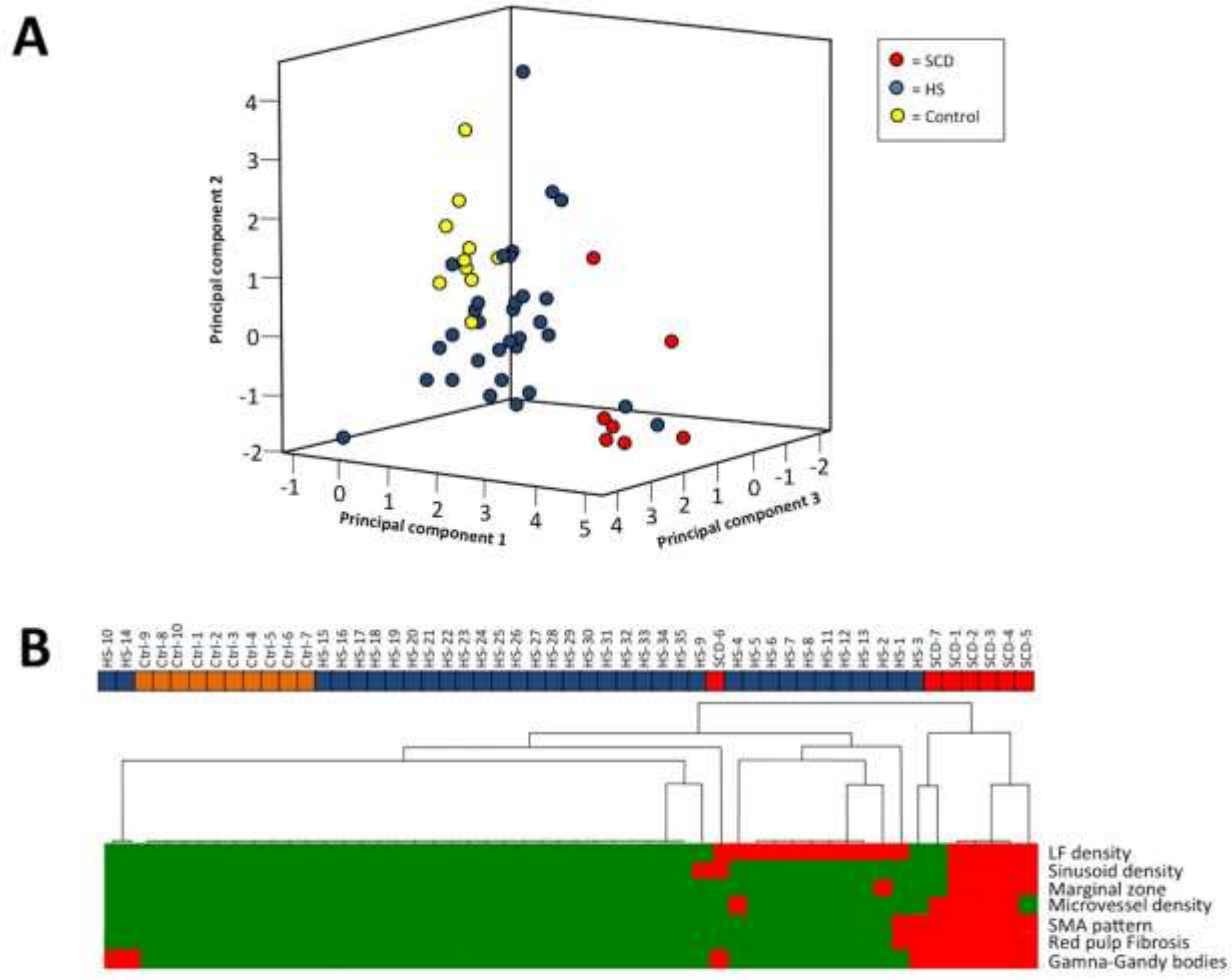

Pizzi M *et al*- Figure 4

Table 1. Clinical-epidemiological and histological features of the studied spleens

	Hereditary Spherocytosis	**Sickle Cell Disease**	**Control Spleens**	**HS vs SCD** (p value)	**HS vs Ctrl** (p value)	**SCD vs Ctrl** (p value)
Mean age at splenectomy (years)	8.7 ±1.2	6.4 ±1.7	9.6 ±3.4	n.s	n.s	n.s
Mean spleen weight (gr)	381.3 ±74.7	427.6 ±167.3	130.6 ±40.7	n.s	<0.01	0.03
Lymphoid follicle density (no/mm^2)	0.3 ±0.03	0.1 ±0.06	0.6 ±0.10	<0.01	<0.01	<0.01
CD8-positive sinusoid density (no/HPF)	47.3 ±7.1	26.2 ± 17.5	57.4 ±2.9	<0.01	<0.01	<0.01
CD34-positive vessel density (no/HPF)	43.5 ±7.7	64.3 ±24.3	45.2 ±2.7	0.04	n.s.	0.05
Gamna-Gandy bodies	1/35	7/7	0/10	<0.01	n.s	<0.01
Presence of white pulp marginal zones	34/35	2/7	10/10	<0.01	n.s.	<0.01
Presence of red pulp fibrosis	2/35	6/7	0/10	<0.01	n.s.	<0.01
Increased SMA-positive myoid cells	2/35	6/7	0/10	<0.01	n.s	<0.01
Red pulp macrophage density (no/HPF)*	64.1±1.3	66.0 ± 2.0	65.3 ±3.3	n.s	n.s	n.s

* the number of red pulp macrophages was assessed by CD68 immunohistochemical stain.

Note: Ctrl= control HPF= high-power field; HS= hereditay spherocytosis; SCD= sickle cell disease

Table 2. Thresholds for the assessment of the histological score (k-means algorithm)

	score 0	**score 1**
Lymphoid follicle density	≥ 0.2	< 0.2
CD8-positive sinusoid density	≥35.9	<35.9
CD34-positive vessel density	<56.5	≥56.5
Fibrosis	Absent	Present
Marginal zones	Present	Absent
Gamna-Gandy bodies	Absent	Present
SMA pattern	Normal	Increased